catalysts

MDPI

Article

Impact of Lubricant Additives on thePhysicochemical Properties and Activity of Three-Way Catalysts

Chao Xie [1,†], Todd J. Toops [1,*], Michael J. Lance [1], Jun Qu [1], Michael B. Viola [2], Samuel A. Lewis [1], Donovan N. Leonard [1] and Edward W. Hagaman [1]

1 Oak Ridge National Laboratory,1 Bethel Valley Rd., Oak Ridge, TN 37831, USA; lancem@ornl.gov (M.J.L.); qujn@ornl.gov (J.Q.); lewissasr@ornl.gov (S.A.L.); leonarddn@ornl.gov (D.N.L.); hagamanew@ornl.gov (E.W.H.)

2 General Motors, Inc., Warren, MI 48093, USA; michael.b.viola@gm.com

* Correspondence: toopstj@ornl.gov; Tel.: +1-865-9461-207

† Currently at Tenneco, Inc., Grass Lake, MI 49240, USA; cxie1@tenneco.com.

Academic Editors: Jae-Soon Choi and Petr Kočí

Received: 1 February 2016; Accepted: 14 March 2016; Published: 4 April 2016

Abstract: As alternative lubricant anti-wear additives are sought to reduce friction and improve overall fuel economy, it is important that these additives are also compatible with current emissions control catalysts. In the present work, an oil-miscible phosphorous-containing ionic liquid (IL), trihexyltetradecylphosphonium bis(2-ethylhexyl) phosphate ([P_{66614}][DEHP]), is evaluated for its impact on three-way catalysts (TWC) and benchmarked against the industry standard zinc-dialkyl-dithio-phosphate (ZDDP). The TWCs are aged in different scenarios: neat gasoline (no-additive, or NA), gasoline+ZDDP, and gasoline+IL. The aged samples, along with the as-received TWC, are characterized through various analytical techniques including catalyst reactivity evaluation in a bench-flow reactor. The temperatures of 50% conversion (T50) for the ZDDP-aged TWCs increased by 30, 24, and 25 °C for NO, CO, and C_3H_6, respectively, compared to the no-additive case. Although the IL-aged TWC also increased in T50 for CO and C_3H_6, it was notably less than ZDDP, 7 and 9 °C, respectively. Additionally, the IL-aged samples had higher water-gas-shift reactivity and oxygen storage capacity than the ZDDP-aged TWC. Characterization of the aged samples indicated the predominant presence of $CePO_4$ in the ZDDP-aged TWC aged by ZDDP, while its formation was retarded in the case of IL where higher levels of $AlPO_4$ is observed. Thus, results in this work indicate that the phosphonium-phosphate IL potentially has less adverse impact on TWC than ZDDP.

Keywords: three way catalysts; phosphorus deactivation; ZDDP; ionic liquid; lubricant additive

1. Introduction

Lubricant improvements are being widely used in the automotive industry to enhance the durability and fuel efficiency of internal combustion engines. In general, commercial lubricants are comprised of base stocks and several categories of additives, such as detergent, dispersant, anti-oxidant, anti-wear, friction modifier, and viscosity modifier. With high effectiveness in wear protection, zinc dialkyl dithiophosphate (ZDDP) is the most common anti-wear additive used in the automotive industry. The major drawback of ZDDP is that it can form ash during combustion and poison emissions control catalysts [1–11]. Thus, there is significant interest in developing a new lubricant additive that is ashless, has less impact on engine emissions control catalysts, and reduces friction and wear. An emerging alternative to ZDDP is oil-miscible ionic liquids (ILs). Recent efforts by Qu *et al.* have developed a group of fully oil-miscible phosphonium-phosphate ILs as next-generation anti-wear additives [12–16]. In addition to excellent oil-miscibility, these ILs also demonstrate a number of other features, such as high thermal stability, non-corrosiveness, excellent wettability on metal

surfaces, and effective anti-scuffing/anti-wear functionality [12–16]. For example, Qu *et al.* [13] have reported that, upon a 1 wt% addition of IL into a synthetic base oil, scuffing failure observed in the case of neat base oil and the base oil plus 1 wt% ZDDP did not occur, and the friction coefficient and wear rate were significantly reduced. Most importantly, a prototype low-viscosity IL-additized engine oil has demonstrated improved fuel economy in standard fuel efficiency engine dynamometer tests [16]. The oil-miscible IL used in this study was trihexyltetradecylphosphonium bis(2-ethylhexyl) phosphate ([P66614][DEHP]). The molecular structures of both ZDDP and this IL are shown in Figure 1. More details regarding the preparation protocols for ILs and their physicochemical properties can be obtained from previous studies [12–15].

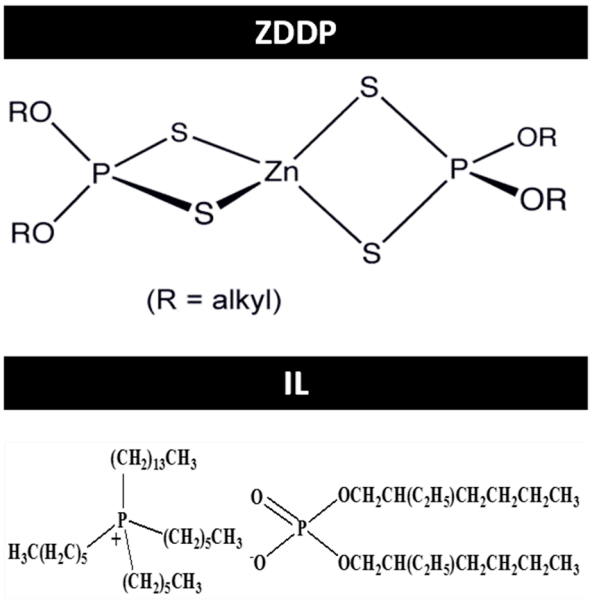

Figure 1. Molecular structures of ZDDP and IL.

The aforementioned information clearly reflects that pronounced progress has been made towards developing highly efficient ILs for engine applications. However, the compatibility of ILs with emissions control systems is unknown. In order to address this question, an accelerated aging routine was implemented starting with a three-way catalyst (TWC) that had been thermally aged to 150,000 miles, or the equivalent of full useful life (FUL) as defined by our partners at General Motors (GM). These thermally-aged TWCs have only been exposed to a nominal level of lubricant additive and, thus, additional exposure is required using the two lubricant additives, ZDDP and IL, to reach FUL exposure of the lubricant additives. For completeness, catalyst aging in the absence of lubricant additives was conducted for comparison. After aging, the catalytic performance of all of the TWCs was evaluated in a bench-flow reactor. The nomenclature for each of the aged parts is listed below:

- **FUL_AR**: TWC thermally-aged to full useful life, evaluated as-received (AR)
- **FUL_NA**: FUL_AR further aged by neat gasoline with no additive (NA)
- **FUL_ZDDP**: FUL_AR further aged by gasoline mixed with ZDDP
- **FUL_IL**: FUL_AR further aged by gasoline mixed with IL

A variety of analytical techniques, such as powder X-ray diffraction (XRD), electron probe microanalysis (EPMA), Inductively coupled plasma mass spectrometry (ICP-MS), and nuclear magnetic resonance (NMR) were employed to characterize these TWCs before and after aging.

2. Results

2.1. Catalyst Characterization

Figure 2 displays the powder XRD patterns for the inlet (IN) portions of FUL_AR, FUL_NA, FUL_ZDDP, and FUL_IL. Two diffraction peaks are visible at 2θ = 29.4 and 33.8° for FUL_AR(IN), which can be assigned to $Ce_{1-x}Zr_xO_2$ mixed oxide. Moreover, a diffraction peak can be seen at 2θ = 40° resulting from the (111) plane of Pd crystals. It is clear that the XRD pattern of FUL_NA(IN) is very similar to that of FUL_AR(IN), suggesting that thermal aging did not remarkably alter the structural property of the TWC. In addition to $Ce_{1-x}Zr_xO_2$ and Pd, two diffraction peaks appear at 26.5 and 28.6°, indicative of the presence of cordierite residues in the TWC washcoat sample. In these samples, efforts were made to remove the washcoat from the cordierite monolith, but as can be noted by these two peaks, some cordierite remained in two of the samples; these are artifacts, not phase changes associated with aging. As to FUL_ZDDP(IN) and FUL_IL(IN), the XRD pattern of the latter is very similar to FUL_AR(IN), while that of the former is much more complicated. Other than those corresponding to $Ce_{1-x}Zr_xO_2$, cordierite, and Pd, new diffraction peaks occur at 2θ = 26.9, 31.9, and 30.2°. The former two and the last one can be assigned to $CePO_4$ (JCPDS 83-0650) and $Zn_2P_2O_7$ (JCPDS 73-1648), respectively. The incorporation of P from ZDDP into the TWC washcoat can account for the formation of $CePO_4$ in the case of FUL_ZDDP(IN). Since ZDDP contains both Zn and P, their interactions in exhaust gas leads to the formation of $Zn_2P_2O_7$ particles, followed by their deposition on the TWC washcoat surfaces. Comparison of the XRD patterns of FUL_ZDDP(IN) and FUL_IL(IN) elucidates that the formation of $CePO_4$ and $Zn_2P_2O_7$ is preferred in the case of ZDDP aging, but is apparently suppressed for FUL_IL. Based on the Scherrer equation, the crystalline size of Pd for the four TWC samples are calculated and listed in Table 1. The crystalline size of Pd for FUL_AR(IN) is comparable to FUL_NA(IN), both of which are between 35 and 37 nm. This fact suggests that thermal aging alone did not give rise to the pronounced growth of Pd crystals. However, the crystalline size of Pd in FUL_ZDDP(IN) is *ca.* 46 nm, being notably larger than those for FUL_AR(IN) and FUL_NA(IN). The crystalline size of Pd for FUL_IL(IN) is *ca.* 40 nm, which is smaller as compared with FUL_ZDDP(IN). Although these size differences appear to be significant, the overall calculated dispersion of the samples only varies from 2.0% to 2.5%. The key features in these XRD results are that ZDDP-aging results in the formation of $CePO_4$ and $Zn_2P_2O_4$ while IL-aging only indicates a small amount of $CePO_4$. There are no signs of crystalline aluminum phosphate in either sample, but it is possible that an amorphous phase is present.

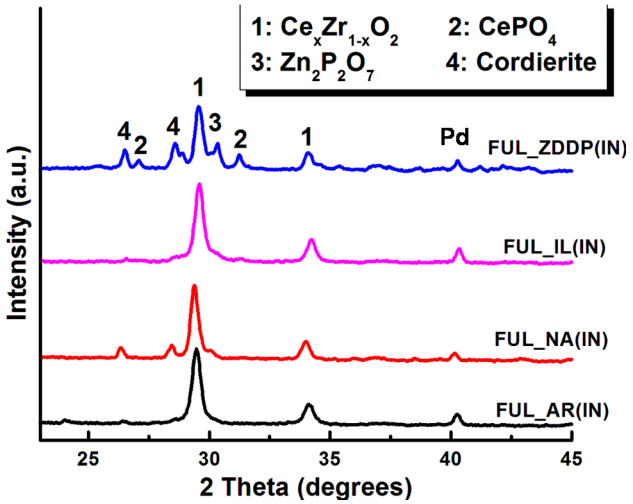

Figure 2. X-ray Diffraction (XRD) patterns for the inlet portion of the three way catalysts (TWCs).

Table 1. Pd Crystalline Sizes for the three way catalysts (TWCs).

Sample	FUL_AR	FUL_NA	FUL_ZDDP	FUL_IL
Crystalline size (nm)	35	36	47	40

In order to investigate the distribution of P and identify its presence in the aged TWCs, EPMA was employed to characterize the TWCs before and after engine aging. Figure 3 displays the EPMA image of FUL_AR(IN) and corresponding EPMA maps for a variety of elements. The cordierite monolith is made of Si and Al (see the Si and Al maps), while the major components for the TWC washcoat are Ce, Zr, and Al (see the Ce, Zr, and Al maps). Figure 3 also indicates an overlayer of P existed on the TWC washcoat surface and sulfur penetrated into the bulk of the TWC washcoat. Both of these originated from the initial engine-based thermal aging at GM where some oil is consumed during the process, but not levels associated with the full-useful-life. Other than these elements, Zn, Ca, and Na are not identified in the FUL_AR(IN) sample. The EPMA maps of P for the inlet, middle, and outlet parts of FUL_NA, FUL_ZDDP, and FUL_IL are presented in Figure 4. In the case of FUL_NA, an overlayer of P can be observed at the inlet similar to FUL_AR(IN) sample, but there is no layer evident in the middle and outlet sections. In contrast, P not only covered the inlet washcoat surfaces of FUL_ZDDP and FUL_IL, but also penetrated into the bulk. Interestingly, an overlayer of P is observed only in the middle and outlet parts of FUL_ZDDP.

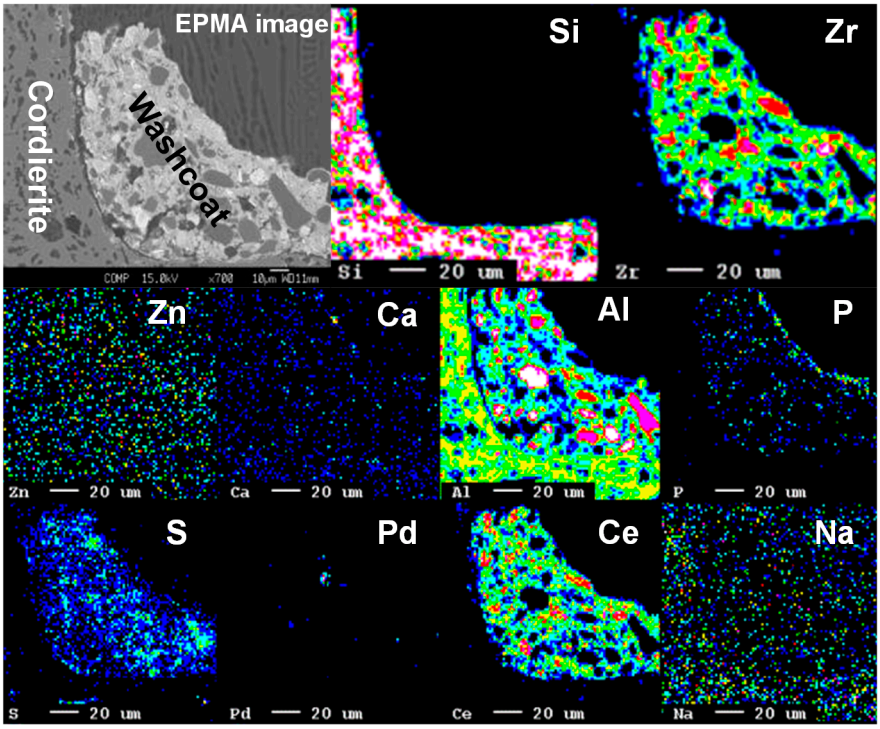

Figure 3. Electron probe microanalysis (EPMA) elemental maps for the inlet of FUL_AR.

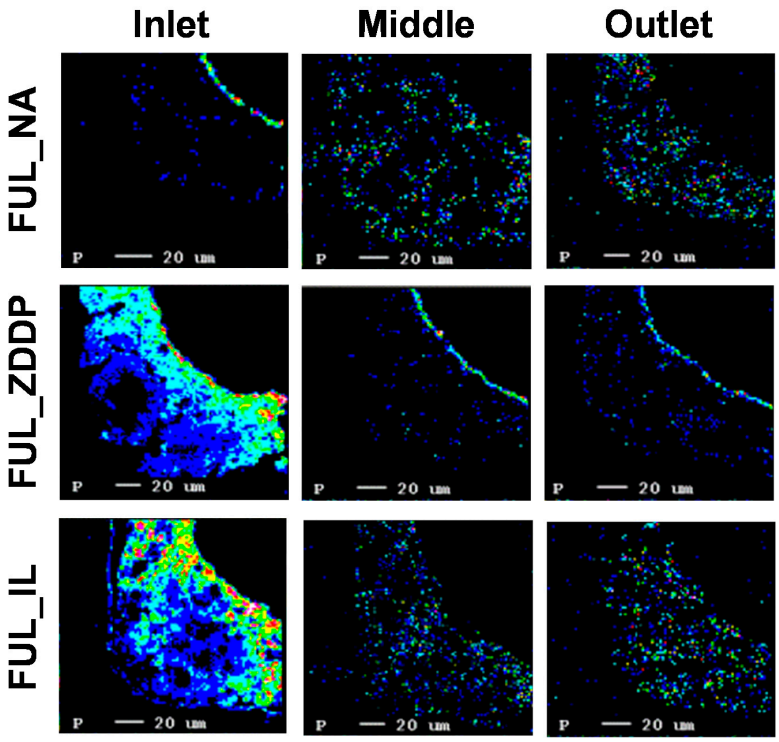

Figure 4. EPMA elemental maps of P for the inlet, middle, and outlet sections of FUL_NA, FUL_ZDDP, and FUL_IL.

To further study the interactions between P and the washcoat of the TWCs, electrospray analysis was performed to analyze the amounts of the P species in TWCs that can be dissolved into water. As can be seen in Figure 5, the concentration of such P species for FUL_IL(IN) is about five times higher than that of FUL_ZDDP(IN). This implies that the IL-based P species are significantly different than those that form with ZDDP. Inductively-coupled plasma mass spectrometry (ICP) was also performed on the sample to obtain a full quantitative analysis of the P in the samples. Figure 6 illustrates that the P level is highest for the ZDDP aged-TWC, but there is a clearly significant P content in the IL-aged TWC. The results shown here are normalized to Pd content as the washcoat loading may vary in thickness in the sample, but the concentration of Pd in the washcoat should remain constant; thus, this normalization routine is a method to account for the washcoat variance.

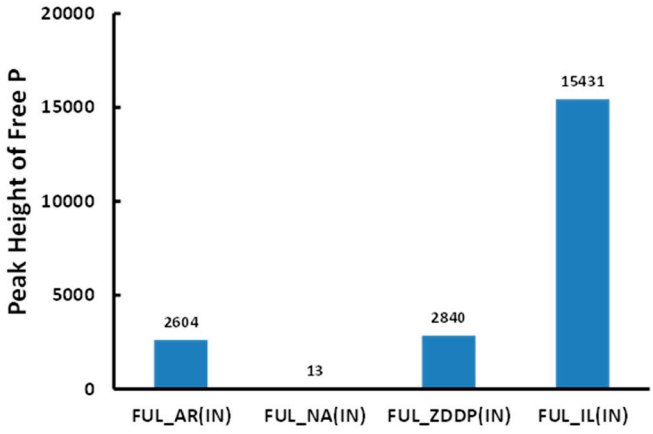

Figure 5. Electrospray analyses of the P species that weakly bond with TWC washcoat.

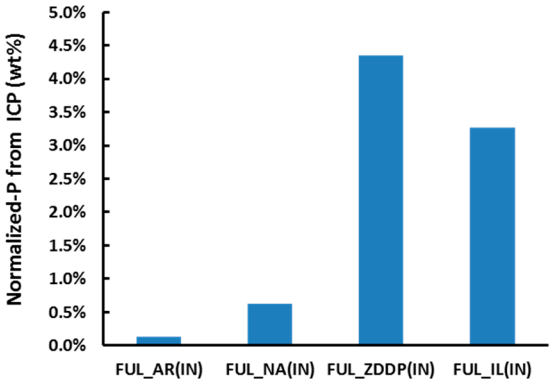

Figure 6. Inductively coupled plasma mass spectrometry (ICP-MS) results for P concentration (normalized to Pd content).

Both EPMA and ICP analysis indicate that the significant presence of P in the washcoat of the inlet of FUL_IL, but XRD could not identify the form of the P species. In order to study the chemical nature of the P species in the TWCs, NMR was used to characterize the inlet of FUL_ZDDP and FUL_IL. Figure 7 exhibits ^{31}P NMR spectra of the inlet parts of FUL_AR, FUL_NA, FUL_ZDDP, and FUL_IL. The NMR response of FUL_AR is very weak, indicating the low P content in the as-received TWC sample. Upon catalyst aging in the absence of lubricant additives, FUL_NA showed a broad peak centered at −5 ppm (discussed below) and a small peak at −30 ppm that is due to $AlPO_4$ [4,10]. The weak $AlPO_4$ peak suggests that the P content in this catalyst sample was low and P largely stayed on washcoat surfaces, in agreement with the EPMA results. Upon catalyst aging in the presence of lubricant additives, both FUL_ZDDP and FUL_IL displayed a strong $AlPO_4$ peak and a broad resonance that extends over the −10 to −20 ppm region. The $AlPO_4$ peak illustrates that during catalyst aging in the presence of lubricant additives P significantly penetrated into the TWC washcoat and reacted to form $AlPO_4$. However, XRD results do not show evidence supporting the formation of $AlPO_4$ in FUL_ZDDP and FUL_IL, suggestive of the amorphous nature of $AlPO_4$ in these two catalyst samples, also reported elsewhere [10]. It is noteworthy that the $AlPO_4$ resonance for FUL_IL is stronger than that for FUL_ZDDP. Quantitative analysis indicates that there is about 10% more $AlPO_4$ in FUL_IL compared with FUL_ZDDP. This fact suggests that, in IL aging, P may prefer to react with aluminum in the DOC washcoat to form $AlPO_4$, thus reducing its negative impact on cerium, *i.e.*, suppressed formation of $CePO_4$ in FUL_IL, as indicated by XRD. This result cannot be corroborated by direct observation of the ^{31}P NMR spectrum of $CePO_4$ since the unpaired electron on the metal in $CePO_4$ causes efficient electron-nuclear relaxation, preventing the detection of a high resolution ^{31}P NMR spectrum of $CePO_4$.

Separate ^{1}H-^{31}P cross-polarization magic angle spinning (CP/MAS) experiments (not shown) on FUL-IL establish that the broad resonance band centered at −10 ppm and, by extension, the similar resonances in the FUL_ZDDP spectrum and the −5 ppm resonance in FUL_NA spectrum, arise from a protonated phosphate group that, on a chemical shift basis, is the dihydrogen phosphate ($H_2PO_4^-$) species [17]. A smaller contribution from the hydrogen phosphate species (HPO_4^{2-}) with chemical shifts centered near −20 ppm may contribute to the FUL-IL and FUL-ZDDP spectra.

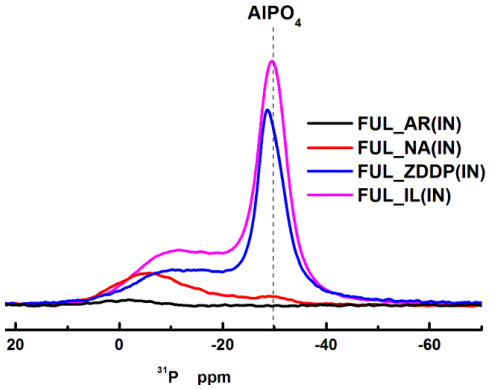

Figure 7. ^{31}P NMR (nuclear magnetic resonance) spectra of the inlet parts of FUL_AR, FUL_NA, FUL_ZDDP, and FUL_IL.

2.2. Catalyst Performance

Figure 8 exhibits the light off curves from heating the inlet samples of the TWCs to 600 °C while flowing a stoichiometric concentration of O_2, 1.59% in this case. The catalytic behavior observed is very typical of TWCs as nearly a step increase in reactivity is observed as the three primary reactants rise from 0% conversion to nearly 100% conversion over a narrow temperature window. To compare the reactivity of the catalysts, a temperature of 50% conversion, T50 is typically reported. Figure 9 displays the T50 for NO, C_3H_6, and CO for FUL_AR(IN), FUL_NA(IN), FUL_ZDDP(IN), FUL_IL(IN), FUL_ZDDP(MI), and FUL_IL(MI). For each reactant the T50 is highest for the ZDDP-aged inlet sample while the IL-aged samples have lower T50s and are, thus, less-impacted. This data also shows that the thermal cycling that occurred during this aging procedure did have a small effect as the no-additive TWC (FUL_NA) had a higher T50 than the as-received case (FUL_AR). Additionally, the middle samples illustrate that the impact of lubricant additives are less significant in both cases further down the flow path.

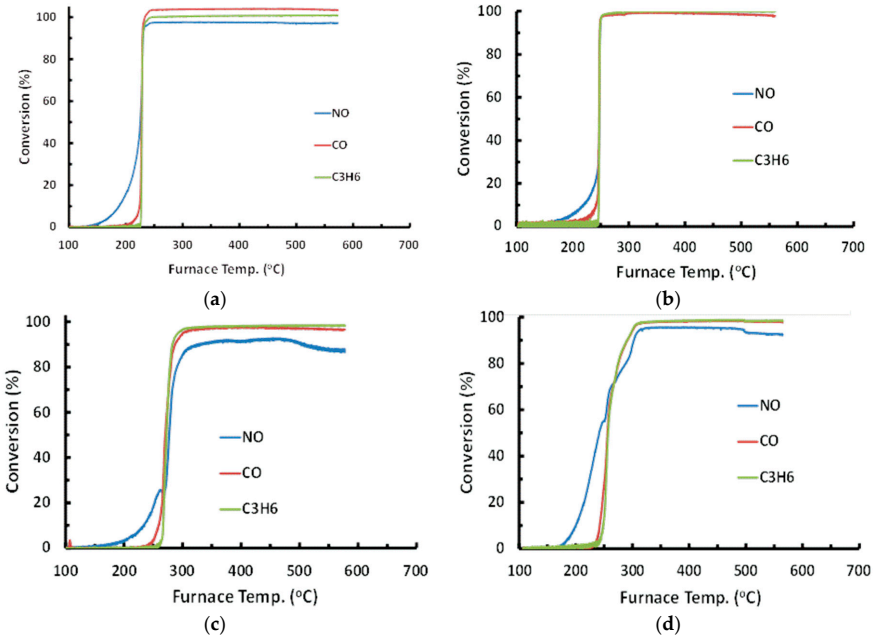

Figure 8. Light off curves of the TWC inlet samples for (**a**) FUL_AR, (**b**) FUL_NA, (**c**) FUL_ZDDP, and (**d**) FUL_IL with a ramp rate of 2 °C/min; furnace temperature is within 5 °C of the inlet gas temperature.

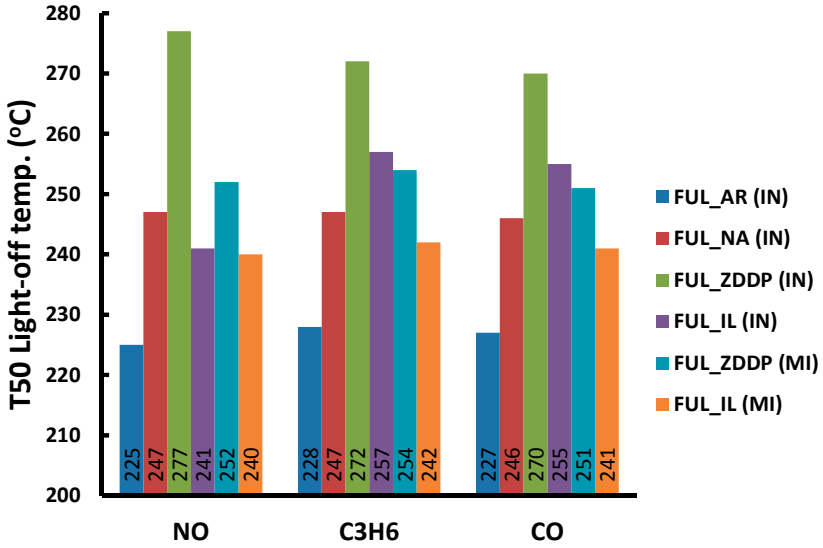

Figure 9. T50 light-off temperatures of NO, C_3H_6, and CO for FUL_AR(IN), FUL_NA(IN), FUL_ZDDP(IN), FUL_IL(IN), FUL_ZDDP(MI), and FUL_IL(MI).

Another important reaction that occurs over TWC is the water-gas-shift (WGS) reaction, where $CO + H_2O \rightarrow CO_2 + H_2$. This reaction is an effective pathway to convert CO to H_2 and, thus, reduce CO emissions even when operating under fuel-rich conditions, and is often very sensitive to aging. Thus, the steady-state WGS reactivity of the aged TWC inlet samples were evaluated at 550 °C and the results are exhibited in Figure 10. The CO conversion for FUL_AR is 13.6%, and is the highest of the evaluated TWCs. This is followed by the FUL_NA at 10.1%. This slight decrease in reactivity further confirms that additional thermal aging occurred during the engine aging in this study. For the TWCs aged by ZDDP and IL, the CO conversion for is 0.9% and 5.8%, respectively. Thus, the additives have a significant effect on the reactivity with the TWCs being significantly more affected by ZDDP than IL.

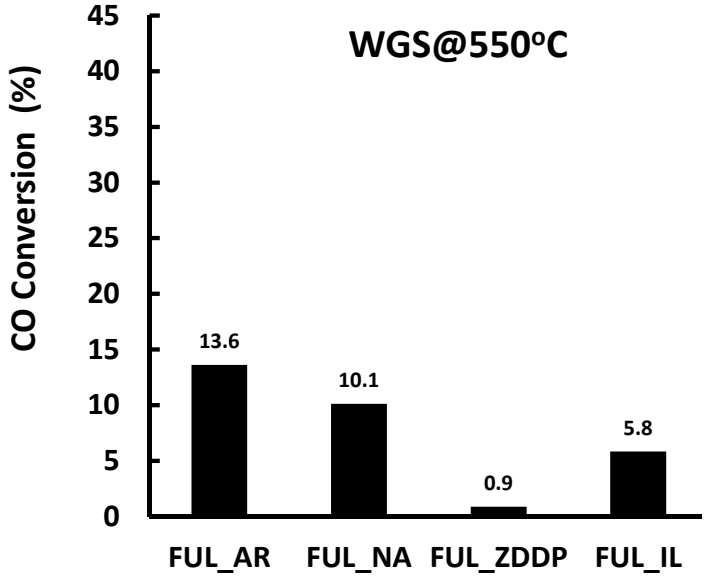

Figure 10. Steady-state CO conversion in WGS for the inlet TWC samples: FUL_AR, FUL_NA, FUL_ZDDP, and FUL_IL at 550 °C.

Finally, the oxygen storage capacity (OSC) of the TWCs was evaluated to specifically measure the effect of the additives on the ceria phase. Ceria has been widely used to improve the functionality

of TWCs due largely to its oxygen storage/release property. Generally, exhaust stoichiometry from automotive gasoline engines dithers rapidly between oxidative and reductive atmospheres. On one hand, in a reductive atmosphere Ce^{3+} can be reduced to Ce^{3+} with the release of highly reactive oxygen species (e.g., 2 $CeO_2 \rightarrow Ce_2O_3 + ½\ O_2$). On the other hand, the presence of excess oxygen will oxidize Ce^{3+} back to Ce^{4+} ($Ce_2O_3 + ½\ O_2 \rightarrow 2\ CeO_2$) resulting in oxygen storage in an oxidative atmosphere. In a reductive atmosphere, the oxygen stored in ceria can be released to assist the oxidation of CO and unburned hydrocarbons in gasoline engine exhaust to CO_2. It is apparent that there exists a mutual conversion cycle between Ce^{4+} and Ce^{3+}, which can effectively buffer against lean and rich conditions to stabilize the performances of TWCs in real vehicle operation. Figure 11 shows the OSC of the inlet samples of FUL_AR, FUL_NA, FUL_ZDDP, and FUL_IL between 300 and 500 °C at a 50 °C interval. For all of the TWC samples their OSCs increase with increasing temperature, and once again it is observed that the ZDDP-aged TWC is most affected during aging while in the IL-aged sample has similar OSC as the no-additive sample (FUL_NA). Also evident in this evaluation is the sharp decrease in overall OSC compared to the as-received case (FUL_AR) illustrating that both phosphorus and thermal aging results in lost OSC from cerium phosphate formation and decreased access to surface sites.

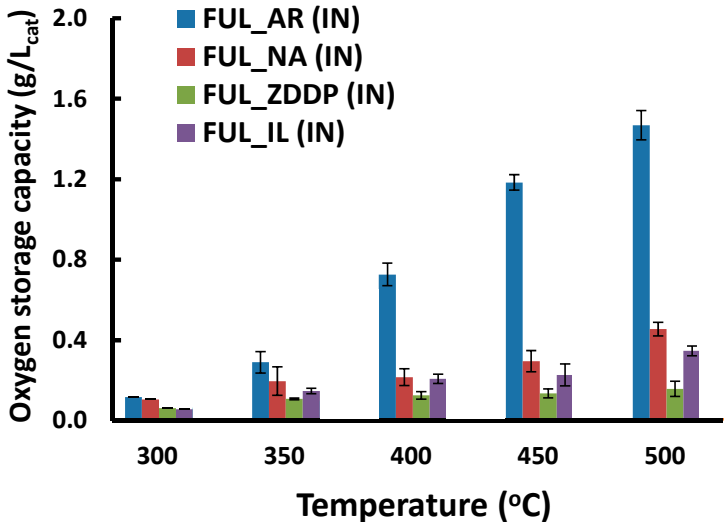

Figure 11. Oxygen storage capacity (OSC) for FUL_AR, FUL_NA, FUL_ZDDP, and FUL_IL.

3. Discussion

As a new category of lubricant additives, ILs are attractive for the automotive industry due to their numerous advantages, such as high thermal stability, non-corrosiveness, excellent wettability, and most importantly effective anti-scuffing/anti-wear and friction reduction characteristics [12–16]. One of the unresolved questions for the practical applications of this technology is the potential impact on TWC reactivity, and how the impact compares with commercially available lubricant additives, such as ZDDP. From prior studies, it is well-known that ZDDP contributes to the deactivation of TWCs through normal oil consumption in engines [1–9]. Vehicle manufacturers must then design the emissions control systems to tolerate some level of Zn and P deactivation over the lifetime of the vehicle such that it still meets emission standards at the end of full useful life.

As a well-known phenomenon, P poisoning is an accumulative, irreversible deactivation process on emissions control catalysts, such as TWCs. P can either form an overlayer on TWC washcoat surfaces to block catalytically-active sites, or penetrate into the bulk of the TWC washcoat and react directly with the washcoat components to form stable compounds such as $CePO_4$. The formation of $CePO_4$ in aged TWCs has been reported in previous studies and has been clearly observed in this study when aging with ZDDP. Elsewhere, Larese *et al.* [18] investigated the contaminants present

in a TWC aged under real working conditions of *ca.* 30,000 km, and demonstrated the formation of $CePO_4$ in the aged catalyst with the aid of XRD. It has been clarified that the formation of $CePO_4$ takes place when a large amount of P is incorporated into TWCs. Granados *et al.* [19] investigated the chemical nature of P-containing species incorporated into ceria, and clarified the effect of P/Ce ratios on the structure and surface properties of phosphated ceria. Their study illustrates that there may exist two different domains for phosphated ceria depending on the P/Ce ratio. Isolated orthophosphate (*i.e.*, PO_4) is the only P species present on the surface and in the subsurface region of phosphated ceria at a lower concentration of P (e.g., P/Ce < 0.03) in TWCs. With the further increase of the P concentration (e.g., P/Ce > 0.03), the surface and subsurface regions of phosphated ceria become saturated by the isolated orthophosphate species such that $CePO_4$ crystals start to nucleate and grow in phosphated ceria. Accordingly, it is reasonable to infer that the concentration of P in a ZDDP-aged TWC is sufficiently high (4.3 wt% from ICP data in Figure 6) leading to the formation of $CePO_4$ in the XRD pattern (Figure 2). However, it is interesting to note that the results in this study indicate the phosphorus-containing IL does not have a significant detectable crystalline $CePO_4$ in the XRD pattern, even though ICP analysis indicates 3.3 wt%.

XRD results also indicate the formation of $Zn_2P_2O_7$ in FUL_ZDDP(IN), which can physically cover TWC washcoat surfaces and block their catalytically-active sites, such as Pd particles. As a consequence, $Zn_2P_2O_7$ may not only impair the OSC of ceria, but also inhibit the adsorption and activation of CO, C_3H_6, and NO on TWCs for their conversion. Thus, the ZDDP-aged TWC has another deactivation mechanism that is not a factor for the IL-aged samples.

Another key difference between ZDDP and IL interactions with the TWC is the NMR results that indicate higher levels of $AlPO_4$ in the IL-aged samples (Figure 6). This, in addition to the high water solubility of P in the IL-aged samples (Figure 5) clearly point to a physicochemical difference in the way the two additives interact with the TWC. The water solubility also indicates that a significant amount of the P in the IL sample is not strongly bound to the TWC and, thus, the metal support interactions that impact catalytic performance are not as strongly affected in the IL case. All of these results indicating different interactions with the TWC were surprising since it was suspected that once the ZDDP- or IL-additive is exposed to combustion conditions in the engine cylinder, the form of the P-containing compound would be similar. However, it seems the lack of metal, such as Zn, in close proximity to the P in the additive has a role in how the P interacts with the TWC components, specifically with respect to forming $CePO_4$, and consequently impacting the TWC reactivity for both emission reduction and water gas shift activity. In the end, it can be concluded that the IL-based lubricant additive employed in this study has less of an impact on TWC functionality than ZDDP additives and, thus, can continue to be considered for commercial viability.

4. Materials and Methods

4.1. Accelerated Catalyst Aging System

The schematic of the catalyst aging system is shown in Figure 12. A 3500W single-phase Briggs and Stratton gasoline genset was used, the frequency and displacement of which are 60 Hz at 3600 rpm and 250 cc, respectively. An oxygen sensor was installed before the TWCs to monitor the oxygen level in the exhaust and, more specifically, the air-to-fuel ratio. The engine operates significantly fuel-rich during its normal operation, while in commercial use TWCs are primarily exposed to stoichiometric air-to-fuel ratios, although fast rich/lean oscillations are common. Thus, to more closely capture conditions of operation, additional air was introduced to the exhaust in front of the TWC allowing the air-to-fuel ratio to oscillate between rich and lean conditions; the period employed was 30 min. lean and 30 min rich for a net stoichiometric exposure. Purely stoichiometric conditions were not possible in this system since the temperature in the catalyst was >1100 °C due to the high concentrations of unburned fuel.

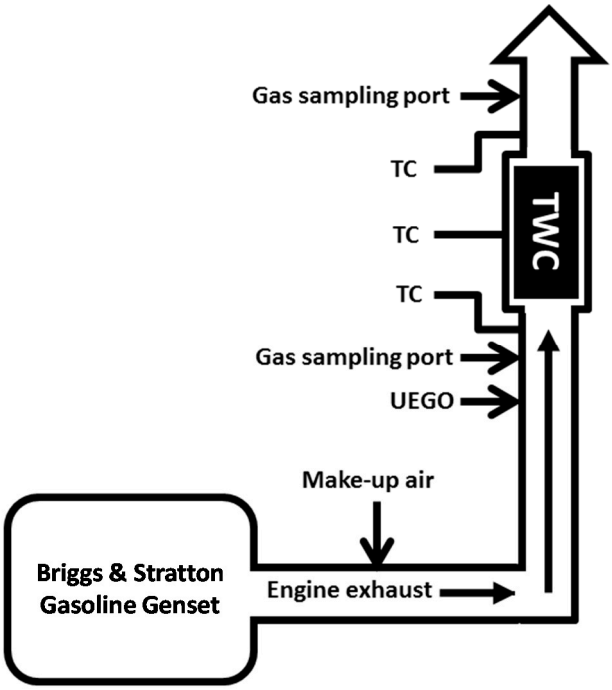

Figure 12. Schematic of the accelerated catalyst aging system using a gasoline genset.

Two thermocouples were used to determine the exhaust temperatures before and after the TWC, and a thermocouple was inserted into the TWCs to monitor the mid-point catalyst temperatures. Gasoline (ORNL fleet fuel) was blended with the lubricant additive introduced to the genset via the engine's carburetor to generate exhaust gases containing decomposition products of lubricant additives, which went through the exhaust pipe to reach the TWCs for aging. About 35 g of ZDDP (Lubrizol, Wickliffe, OH, USA) or IL (synthesized as described elsewhere [12–15]) was used in each catalyst aging evaluation to simulate the maximum lifetime consumption of lubricant anti-wear additive in a modern automotive engine (90 mg/km) . This consumption rate is conservatively based on the high end of "normal" oil consumption data from vehicle operation using the standard road cycle [20]. The estimate also assumes 1% additive concentration in the lubricant.

As shown in Figure 13 (step A), a close-coupled TWC was provided by GM that has a two-zone catalyst layer with a different formulation in the front ~1/3 compared to the rear. The TWC has been thermally aged to 150,000 miles, or the equivalent of full useful life (FUL) as defined by our partners at GM; thus, it is expected to be in such a state that is most sensitive to catalyst poisoning caused by phosphorus (P)-containing lubricant additives such as ZDDP and IL. Three catalyst cores (42 mm OD and 155 mm long) were extracted from the FUL-aged TWC for additive exposure, as demonstrated by Figure 13 (step B). FUL_NA, FUL_ZDDP, and FUL_IL are used in this study to represent the aged TWCs, which stand for the TWC aged by neat gasoline with no additive, gasoline+ZDDP, and gasoline+IL, respectively. The purpose of catalyst aging in the absence of lubricant additive is to clarify the impact of the additional thermal aging on TWCs during the additive exposure. The as-received TWC (FUL_AR) was also investigated in this study as the baseline. Each TWC sample was mounted in an exhaust can (Figure 13, step C) for engine aging. Before being placed in the exhaust can, the catalysts were wrapped in a vermiculite-coated fiber mat which provided insulation and prevented gas slippage around the TWC cores.

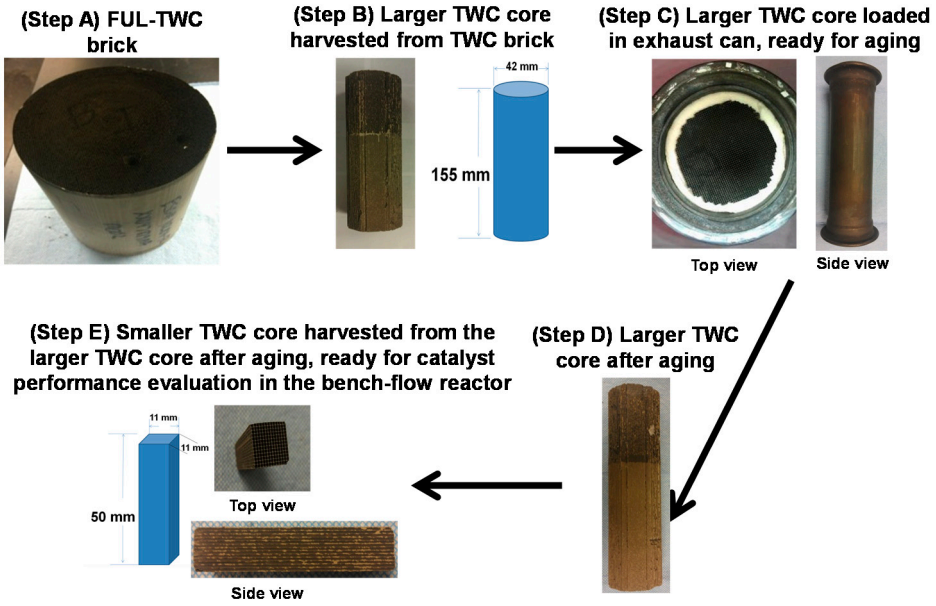

Figure 13. Sample preparation steps for engine aging and catalyst evaluation in bench-flow reactor.

Our target was to conduct TWC aging at about 900 °C for the mid-point catalyst temperature with 950 °C being the maximum, which made it impossible to operate the TWC under stoichiometric conditions during aging. This was due to the existence of >5% CO in the exhaust and, thus, with the addition of a stoichiometric level of O_2 in front of the TWC, results in a large exotherm and a mid-bed temperature >1100 °C. As a result, catalyst aging was conducted by altering the operation between lean and rich in such a way that the total time on rich matched that on lean. The switch between rich and lean was achieved through changing the flow rate of make-up air. For the catalyst aging tests, 28.4 L of gasoline without or with the addition of lubricant additives (about 35 g) was consumed in a time period of more than 20 h. Afterwards, 1.9 L of neat gasoline was added and consumed to ensure a minimum level of lubricant additives left behind. During the catalyst aging process, engine exhaust gases were analyzed before and after TWCs to provide an initial determination of the impact of the lubricant additives on the TWC performances. CAI (California Analytical Instruments) 602P digital analyzer was used to monitor the concentrations of CO_2, CO, and O_2, and a CAI 400-HCLD was used to measure NO_x in exhaust gases.

4.2. Catalyst Characterization

In order to fully evaluate the impact of lubricant additives on TWCs, a number of analytical techniques were used in this study to characterize the catalysts before and after aging. These techniques include XRD , NMR , and EPMA . The characterization results are expected to help better understand how the different lubricant additives affect the physicochemical properties of TWCs. For XRD and NMR, TWC washcoat was separated from cordierite and sieved to minimize the adverse impact of cordierite on the characterization results.

The XRD patterns were recorded by Panalytical Xpert diffractometer using Cu Kα radiation and X'Celerator detector . All scans used 1/4° fixed slits and a 1/2° anti-scatter slit. The crystalline size D was calculated with the aid of the Scherrer equation: $D = 0.94\lambda/(\beta\cos\theta)$, where λ is the wavelength of the X-ray (λ = 0.154 nm), θ is the Bragg's angle, and β is the width of the line at the half-maximum intensity. EPMA was used to determine the location and concentration of various elements in the TWCs before and after aging. Elemental micrographs were obtained from a SX-50 camera device with four crystal-focusing spectrometers for wavelength-dispersive X-ray spectroscopy (WDS). To prepare the samples for EPMA analysis, the TWC catalysts were sectioned into small samples no larger than 1.5 cm in diameter and 1 cm in length. The samples were placed into phenolic rings and covered

in a resin to secure them in place. After the resin hardened, each sample was carefully polished to ensure a flat, smooth surface for EPMA analysis. For electrospray analysis, roughly 100 mg of catalyst sample was obtained from the front inlet of the TWCs before and after engine aging. The catalyst sample was submerged into a beaker of water, which was put in a sonicator to help dissolve the P species that weakly bond with the TWC washcoat. The P species that can dissolve into water were analyzed by electrospray coupled with MS. NMR was performed using a Bruker Avance 400 (B0 = 9.4T) spectrometer at a resonance frequency of 104.2 MHz and a spinning speed of 10 kHz. ICP analysis was performed by Galbraith Laboratories.

4.3. Catalyst Performance Evaluation

As shown in Figure 13 (steps D and E), smaller TWC cores (11×11×50 mm) were harvested from the larger TWC cores for catalyst evaluation in a bench-flow reactor . The inlet parts of all four catalysts (*i.e.*, FUL_AR, FUL_NA, FUL_ZDDP, and FUL_IL) and the middle parts of FUL_ZDDP, and FUL_IL were evaluated in the present work. IN and MI sections were used to differentiate the inlet and middle parts. For example, FUL_ZDDP(IN) and FUL_ZDDP(MI) represent the inlet part and middle part of FUL_ZDDP, respectively. Catalytic performance evaluations were performed using a laboratory bench-flow reactor, as described in more detail elsewhere [21]. Briefly, the TWC cores were tightly wrapped using insulation tape and inserted into a horizontal quartz tube reactor , which was heated using a horizontal bench-top furnace (Lindberg/Blue M) . In order to simulate gasoline engine exhaust gases, the reaction feed stream contained C_3H_6, CO, NO, O_2, H_2, H_2O , CO_2, and N_2. All gases were provided by Air Liquide (Oak Ridge, TN, USA). The gas hourly space velocity (GHSV) during the reaction was maintained at 75,000 h^{-1}. Mass flow controllers were used to feed the gases and a high performance liquid chromatography (HPLC) pump was used to feed the water. The reaction feed stream was preheated and water was pre-evaporated by a cylindrical oven that was placed upstream the catalyst bed. The front part of the quartz tube reactor was filled with quartz beads to preheat the feed gases to ensure proper mixing and uniform heating of the incoming gases. The TWC performances as a function of air-to-fuel ratios (AFRs) were examined in the presence of 0.1% C_3H_6, 1.8% CO, 0.12% NO, 0.6% H_2, 5% H_2O, 5% CO_2, N_2 balance, and variable concentrations of O_2 from 1.0 to 1.64%. In order to measure the light-off temperatures for the conversion of NO, CO, and C_3H_6, the reaction temperature was increased from 100 to 550 °C at a ramp of 2 °C/min in the presence of 0.1% C_3H_6, 1.8% CO, 0.12% NO, 1.59% O_2, 0.6% H_2, 5% H_2O, 5% CO_2, and N_2 balance. The steady-state performances of the TWCs for the water-gas-shift reaction (WGS: CO + H_2O → H_2 + CO_2) were evaluated at 550 °C with the reaction feed stream being 1.8% CO, 5% H_2O, and N_2 balance. The oxygen storage capacity (OSC) of the TWCs was measured in a temperature range from 300 to 550 °C at a 50 °C interval. The TWC was treated with O_2, followed by switching the reaction gas from O_2 to CO with the generation of CO_2 as a result of the reaction between CO and reactive oxygen species present on the TWC surfaces. The thus-generated CO_2 was quantified and used to calculate the OSC of TWCs. For all the reactions, the compositions of the outlet gases such as NO, NO_2, CO, C_3H_6, CO_2, and H_2O were monitored by an on-line fourier transform infrared spectroscopy (FT-IR) (MKS Multigas 2030 HS) . The temperature and pressure of the infrared spectroscopy (IR) gas cell is 191 °C and 0.99 atm, respectively. The conversion of CO, C_3H_6, and NO was calculated using the following equation:

$$Conversion\ (\%) = \frac{C_{In} - C_{Out}}{C_{In}} \times 100 \quad (1)$$

where C_{In} is the gas concentration in the original feed stream before TWCs, and C_{Out} is the gas concentration after TWCs.

5. Conclusions

The present work was carried out to clarify the impact of lubricant additives (ZDDP *vs* IL) on the physicochemical properties of TWCs and their catalytic performance in engine emissions control.

In comparison with ZDDP, IL-aged TWCs were moderately more reactive for emissions control of $CO/NO_x/C_3H_6$, had higher water-gas-shift reactivity, and more oxygen storage capacity. The primary materials differences in the aged TWCs were the following:

- ZDDP-aged TWCs had significantly higher concentrations of crystalline $CePO_4$ and Zn_2PO_7 while neither species was measured in the IL-aged TWC
- The primary detected P-compound on the IL-aged TWC was $AlPO_4$; additionally, there is a significant water soluble P-species on the IL-aged TWC that is not present in the ZDDP-aged TWC
- The overall P content on the IL-aged TWCs was 33% lower than the ZDDP-aged TWC

Therefore, it can be concluded that the studied IL ([P66614][DEHP]), when used as an engine oil additive, has potentially less adverse impact on TWC functionality than the conventional ZDDP.

Acknowledgments: Research was sponsored by the Vehicle Technologies Office, Office of Energy Efficiency and Renewable Energy, US Department of Energy (DOE). The authors gratefully acknowledge the support and guidance of program managers Kevin Stork and Steve Przesmitzki at DOE. The authors thank E. Bardasz from Lubrizol for providing the ZDDP. This manuscript has been authored by UT-Battelle, LLC, under Contract No. DE-AC0500OR22725 with the U.S. Department of Energy. The United States Government retains and the publisher, by accepting the article for publication, acknowledges that the United States Government retains a non-exclusive, paid-up, irrevocable, world-wide license to publish or reproduce the published form of this manuscript, or allow others to do so, for the United States Government purposes. The Department of Energy will provide public access to these results of federally sponsored research in accordance with the DOE Public Access Plan (http://energy.gov/downloads/doe-public-access-plan).

Author Contributions: Chao Xie and Todd J. Toops conceived and designed the experiments; Chao Xie, Michael J. Lance, Samuel A. Lewis, Donovan N. Leonard, and Edward W. Hagaman performed the experiments; Chao Xie, Todd J. Toops, Michael J. Lance, Jun Qu, Michael B. Viola, Samuel A. Lewis, Donovan N. Leonard, and Edward W. Hagaman analyzed the data; Michael B. Viola provided the TWCs; Chao Xie and Todd J. Toops wrote the first draft of the paper.

Conflicts of Interest: The authors declare no conflict of interest.

References

1. Williamson, W.B.; Perry, J.; Goss, R.L.; Gandhi, H.S.; Beason, R.E. Catalyst Deactivation Due to Glaze Formation from Oil-Derived Phosphorus and Zinc. *SAE Tech. Pap. Ser.* **1984**. [CrossRef]
2. Culley, S.A.; McDonnell, T. The Impact of Passenger Car Motor Oil Phosphorus Levels on Engine Durability, Oil Degradation, and Exhaust Emissions in a Field Trial. *SAE Tech. Pap. Ser.* **1995**. [CrossRef]
3. Darr, S.T.; Choksi, R.A.; Hubbard, C.P.; Johnson, M.D.; McCabe, R.W. Effects of Oil-Derived Contaminants on Emissions from TWC-Equipped Vehicles. *SAE Tech. Pap. Ser.* **2000**. [CrossRef]
4. Rokosz, M.J.; Chen, A.E.; Lowe-Ma, C.K.; Kucherov, A.V.; Benson, D.; Peck, M.C.P.; McCabe, R.W. Characterization of phosphorus-poisoned automotive exhaust catalysts. *Appl. Catal. B* **2001**, *33*, 205–215. [CrossRef]
5. Uy, D.; O'Neill, A.E.; Xu, L.; Weber, W.H.; McCabe, R.W. Observation of cerium phosphate in aged automotive catalysts using Raman spectroscopy. *Appl. Catal. B* **2003**, *41*, 269–278. [CrossRef]
6. Eaton, S.J.; Nguyen, K.; Bunting, B.G. Deactivation of Diesel Oxidation Catalysts by Oil-Derived Phosphorus. *SAE Tech. Pap. Ser.* **2006**. [CrossRef]
7. Bunting, B.G.; More, K.L.; Sr, S.A.L.; Toops, T.J. Phosphorous Poisoning and Phosphorous Exhaust Chemistry with Diesel Oxidation Catalysts. *SAE Tech. Pap. Ser.* **2005**. [CrossRef]
8. Guevremont, J.M.; Guinther, G.; Jao, T.-C.; Herlihy, T.; White, R.; Howe, J. Development of an Engine-Based Catalytic Converter Poisoning Test to Assess the Impact of Volatile ZDDP Decomposition Products from Passenger Car Engine Oils. *SAE Tech. Pap. Ser.* **2007**. [CrossRef]
9. Bardasz, E.A.; Schiferl, E.; Nahumck, W.; Kelley, J.; Williams, L.; Hubbard, C.P.; Thanasiu, E.; Jagner, M.; O'Neill, A.; Uy, D. Low Volatility ZDDP Technology: Part 2 - Exhaust Catalysts Performance in Field Applications. *SAE Tech. Pap. Ser.* **2007**. [CrossRef]
10. Matam, S.K.; Otal, E.H.; Aguirre, M.H.; Winkler, A.; Ulrich, A.; Rentsch, D.; Weidenkaff, A.; Ferri, D. Thermal and chemical aging of model three-way catalyst Pd/Al_2O_3 and its impact on the conversion of CNG vehicle exhaust. *Catal. Today* **2012**, *184*, 237–224. [CrossRef]

11. Matam, S.K.; Weidenkaff, M.A.N.A.; Ferri, D. Time resolved operando spectroscopic study of the origin of phosphorus induced chemical aging of model three-way catalysts Pd/Al_2O_3. *Catal. Today* **2013**, *205*, 3–9. [CrossRef]
12. Qu, J.; Bansal, D.G.; Yu, B.; Howe, J.; Luo, H.; Dai, S.; Li, H.; Blau, P.J.; Bunting, B.G.; Mordukhovich, G.; Smolenski, D.J. Antiwear Performance and Mechanism of an Oil-Miscible Ionic Liquid as a Lubricant Additive. *ACS Appl. Mater. Interfaces* **2012**, *4*, 997–1002. [CrossRef] [PubMed]
13. Qu, J.; Luo, H.; Chi, M.; Ma, C.; Blau, P.J.; Dai, S.; Viola, M.B. Comparison of an oil-miscible ionic liquid and ZDDP as a lubricant anti-wear additive. *Tribol. Int.* **2014**, *71*, 88–97. [CrossRef]
14. Barnhill, W.C.; Qu, J.; Luo, H.; Meyer, H.M., III; Ma, C.; Chi, M.; Papke, B.L. Phosphonium-Organophosphate Ionic Liquids as Lubricant Additives: Effects of Cation Structure on Physicochemical and Tribological Characteristics. *ACS Appl. Mater. Interfaces* **2014**, *6*, 22585–22593. [CrossRef] [PubMed]
15. Qu, J.; Barnhill, W.C.; Luo, H.; Meyer, H.M.; Leonard, D.N.; Landauer, A.K.; Kheireddin, B.; Gao, H.; Papke, B.L.; Dai, S. Synergistic effects between phosphonium-alkylphosphate ionic liquids and zinc dialkyldithiophosphate (ZDDP) as lubricant additives. *Adv. Mater.* **2015**, *27*, 4767–4774. [CrossRef] [PubMed]
16. Barnhill, W.C.; Gao, H.; Kheireddin, B.; Papke, B.L.; Luo, H.; West, B.H.; Qu, J. Tribological Bench and Engine Dynamometer Tests of a Low Viscosity SAE 0W-16 Engine Oil Using a Combination of Ionic Liquid and ZDDP as Anti-wear Additives. *Front. Mech. Eng.* **2015**, *1*. [CrossRef]
17. West, B.H.; Sluder, C.S. Lubricating Oil Consumption on the Standard Road Cycle. *SAE Tech. Pap. Ser.* **2013**. [CrossRef]
18. Brookshear, D.W.; Nam, J.-G.; Nguyen, K.; Toops, T.J.; Binder, A. Impact of sulfation and desulfation on NO_x reduction using Cu-chabazite SCR catalysts. *Catal. Today* **2015**, *258*, 359. [CrossRef]
19. Nakayama, H.; Hayashi, A.; Tsuhaku, M.; Eguchi, T.; Nakamura, N. Characterization of Polymorphic Cerium Phosphatesas Studied by Solid-State High-Resolution ^{31}P NMR. *Phosphorus Res. Bull.* **1998**, *8*, 89–94. [CrossRef]
20. Larese, C.; Galisteo, F.C.; Granados, M.L.; Mariscal, R.; Fierro, J.L.G.; Furió, M.; Fernández Ruiz, R. Deactivation of real three way catalysts by $CePO_4$ formation. *Appl. Catal. B* **2003**, *40*, 305–317. [CrossRef]
21. Granados, M.L.; Galisteo, F.C.; Lambrou, P.S.; Mariscal, R.; Sanz, J.; Sobrados, I.; Fierro, J.L.G.; Efstathiou, A.M. Role of P-containing species in phosphated CeO_2 in the deterioration of its oxygen storage and release properties. *J. Catal.* **2006**, *239*, 410–421.